Contributions of excitation autoionization to the electron-impact ionization of Mg$^+$, Al^{2+}, and Si^{3+} in the distorted-wave approximation with exchange

D. C. Griffin* and C. Bottcher

Physics Division, Oak Ridge National Laboratory, Oak Ridge, Tennessee 37830

M. S. Pindzola

Department of Physics, Auburn University, Auburn, Alabama 36849
(Received 7 August 1981)

The contributions of excitation autoionization to electron-impact ionization in the Na-like ions Mg$^+$, Al^{2+}, and Si^{3+} are calculated using the distorted-wave approximation with exchange. Inner-shell excitations of the type $2p^63s \rightarrow 2p^53snl$ ($n = 3,4$; $l = 0,1,2$) are included. The calculations indicate that the largest contribution should be due to the $2p \rightarrow 3p$ excitations in all three elements, although the relative importance of this transition decreases with ionic charge. Comparisons of these results with recent experimental measurements indicate that the distorted-wave approximation overestimates the magnitude of the monopole-dominated $2p \rightarrow np$ transitions. Possible reasons for this discrepancy between experiment and theory are discussed, and additional calculations and experiments are suggested.

I. INTRODUCTION

The effects of autoionization on the electron-impact ionization of the members of the Na I isoelectronic sequence have been studied extensively, primarily because of the large contributions that are expected in Fe^{15+}, which is an important ion in astrophysical and laboratory plasmas. Bely[1] calculated the contributions of the transitions

$$2p^63s \rightarrow 2p^53s\,3l \quad (l = 0,1,2)$$

to the ionization of Mg$^+$, Al^{2+}, P^{4+}, Ca^{9+}, and Fe^{15+}. However, his results, which were determined by scaling Coulomb-Born collision strengths for Fe^{16+}, severely overestimate the effects of excitation autoionization. Moores and Nussbaumer[2] considered the transitions

$$2p^63s \rightarrow 2p^53snl \quad (n = 3,4,5; \; l = 0,1,2)$$

in Mg$^+$ using the Coulomb-Born approximation. Unlike Bely whose results indicated that 75% of the effects of autoionization arise from the $2p^63s \rightarrow 2p^53s\,3d$ transitions, they found the largest resonance to be due to the transition $2p^63s \rightarrow 2p^53s\,3p$. In addition, instead of the 100% enhancement predicted by Bely for Mg$^+$, their calculations indicated that the contribution due to autoionization should be approximately 20%. Until now, the only experimental data for this sequence

have been for Mg$^+$ by Martin et al.[3] who did not observe any abrupt increases in the ionization curve, and who estimated that any contributions of autoionization to the ionization cross section should be less than 3.0×10^{-18} cm^2 (or less than 7% in the energy range where the resonances are expected to occur). More recently, Cowan and Mann[4] carried out a detailed study of the contributions of autoionization to the total ionization rates in Fe^{15+} using the distorted-wave approximation with exchange and including the effects of the branching ratio for autoionization versus radiative decay.

Crandall et al.[5] have now measured the ionization cross sections in Mg$^+$, Al^{2+}, and Si^{3+}, and they report their results in the accompanying paper. We have made theoretical calculations of the excitation-autoionization transitions

$$2p^63s \rightarrow 2p^53snl \quad (n = 3,4; \; l = 0,1,2)$$

in Mg$^+$, Al^{2+}, and Si^{3+} using the distorted-wave approximation with exchange, in order to provide a detailed comparison of the experimental and theoretical positions and magnitudes of these resonances.

II. CALCULATIONAL PROCEDURE

If we assume that ionization and excitation autoionization are independent processes then the to-

tal ionization cross section, σ_{total}, is given by the equation

$$\sigma_{\text{total}} = \sigma_{\text{direct}} + \sum_j \sigma^j_{\text{excit}} B^a_j , \tag{1}$$

where σ_{direct} is the cross section for direct ionization, σ^j_{excit} is the excitation cross section of inner-shell electrons to the autoionizing level j, and B^a_j is the branching ratio for autoionization from the level j, which is given by

$$B^a_j = \frac{\sum\limits_m A^a_{jm}}{\sum\limits_m A^a_{jm} + \sum\limits_k A^r_{jk}} , \tag{2}$$

where A^a_{jm} is the autoionization rate to channel m, and A^r_{jk} is the radiative rate to the lower bound level k. For the results given here, the autoionizing rates were calculated using the Hartree exchange method[4,6] for both the continuum and bound-state wave functions; and with the exception of the $2p^63s \rightarrow 2p^53snp$ transitions, the branching ratios were found to be very nearly equal to unity.

With the distorted-wave exchange approximation in the $\mathcal{L}\mathcal{S}$ representation, the excitation cross section for a transition of the form

$$k_i l_i + \alpha_i L_i S_i \rightarrow \alpha_f L_f S_f + k_f l_f$$

is given by

$$\sigma_{\text{excit}} = \frac{\pi a_0^2}{k_i^2 2(2L_i+1)(2S_i+1)} \sum_{\substack{l_i l_f \\ \mathcal{L}\mathcal{S}}} (2\mathcal{L}+1)(2\mathcal{S}+1) \, |\, T(\alpha_i L_i S_i, l_i \mathcal{L}\mathcal{S}; \alpha_f L_f S_f, l_f \mathcal{L}\mathcal{S})\,|^2 , \tag{3}$$

where $L_i S_i$ and $L_f S_f$ represent the total angular momentum and spin of the initial and final bound states, respectively; α_i and α_f represent all other quantum numbers needed to specify the initial and final bound states; $k_i l_i$ and $k_f l_f$ are the wave numbers and orbital angular momenta of the incoming and scattered electrons, respectively; $\mathcal{L}$ and $\mathcal{S}$ are the total orbital and spin angular momenta of the $N+1$ electron system; and $T(\alpha_i L_i S_i, l_i \mathcal{L}\mathcal{S}; \alpha_f L_f S_f, l_f \mathcal{L}\mathcal{S})$ is an element of the transition matrix $\underline{T}$. $\underline{T}$ is related to the reactance matrix $\underline{R}$ by the equation

$$\underline{T} = \frac{-2i\underline{R}}{1 - i\underline{R}} . \tag{4}$$

If the elements of $\underline{R}$ are such that $|R(\alpha_i L_i S_i, l_i \mathcal{L}\mathcal{S}; \alpha_f L_f S_f, l_f \mathcal{L}\mathcal{S})| \ll 1$, then

$$\underline{T} = -2i\underline{R} , \tag{5}$$

where

$$R(\alpha_i L_i S_i, l_i \mathcal{L}\mathcal{S}; \alpha_f L_f S_f, l_f \mathcal{L}\mathcal{S}) = -\langle \Psi(\alpha_i L_i S_i, l_i \mathcal{L}\mathcal{S}) | H - E | \Psi(\alpha_f L_f S_f, l_f \mathcal{L}\mathcal{S}) \rangle \tag{6}$$

and $\Psi(\alpha L S, l \mathcal{L}\mathcal{S})$ is an antisymmetrized, coupled $N+1$ electron wave function, H is the Hamiltonian for the $N+1$ electron system, E is the total energy, and the radial part of the continuum wave functions are normalized to $1/\sqrt{k}$ as $r \rightarrow \infty$. In the approximation that the spin orbitals for the initial and final states of the active bound electron are orthogonal, and the overlap between the one-electron continuum wave functions and the bound-state spin orbitals can be neglected,

$$R(\alpha_i L_i S_i l_i \mathcal{L}\mathcal{S}; \alpha_f L_f S_f l_f \mathcal{L}\mathcal{S}) = -\left\langle \Psi(\alpha_i L_i S_i, l_i \mathcal{L}\mathcal{S}) \left| \sum_{j=1}^N \frac{2}{r_{j,N+1}} \right| \Psi(\alpha_f L_f S_f, l_f \mathcal{L}\mathcal{S}) \right\rangle . \tag{7}$$

In this work, the radial functions of the bound-state spin orbitals were calculated using the Hartree-Fock method with relativistic modifications (HFR),[7] and the continuum wave functions were computed using a semiclassical exchange potential.[8] The elements of the reactance matrix can be derived from standard techniques, and for transitions of the type

$$k_i l_i + 2p^63s \rightarrow 2p^53s\,(^{2S+1}P)nl L_f S_f + k_f l_f \quad (nl \neq 3s)$$

are given by

$$R(\alpha_i L_i S_i, l_i \mathcal{L}\mathcal{S}; \alpha_f L_f S_f, l_f \mathcal{L}\mathcal{S}) = r_d^{L_f} R_d^{L_f}(2pk_i l_i; nl k_f l_f) + \sum_\lambda r_e^\lambda R_e^\lambda(2pk_i l_i; nl k_f l_f) , \tag{8}$$

where

$$r_d^{L_f} = (-1)^{l_f+1} \left[\frac{3(2l+1)(2l_f+1)(2S+1)}{2(2L_f+1)} \right]^{1/2} \begin{bmatrix} 1 & L_f & l \\ 0 & 0 & 0 \end{bmatrix} \begin{Bmatrix} l_i & L_f & l_f \\ 0 & 0 & 0 \end{Bmatrix} \delta_{S_f,1/2}$$ (9)

and

$$r_e^\lambda = (-1)^{l_i+l_f+L_f+1} \left[\frac{3(2l+1)(2l_f+1)(2S+1)(2L_f+1)}{8} \right]^{1/2}$$

$$\times \left[\delta_{S_f,1/2} + 12(-1)^{S+S_f+S+1/2} \left[\frac{2S_f+1}{2} \right]^{1/2} \begin{Bmatrix} \frac{1}{2} & \frac{1}{2} & \mathcal{S} \\ \frac{1}{2} & S_f & 1 \end{Bmatrix} \begin{Bmatrix} \frac{1}{2} & \frac{1}{2} & \mathcal{S} \\ \frac{1}{2} & S_f & 1 \end{Bmatrix} \right]$$

$$\times \left[\begin{bmatrix} 1 & \lambda & l_f \\ 0 & 0 & 0 \end{bmatrix} \begin{bmatrix} l & \lambda & l_i \\ 0 & 0 & 0 \end{bmatrix} \begin{Bmatrix} 1 & l & L_f \\ l_i & l_f & \lambda \end{Bmatrix} \right]$$ (10)

and where R_d and R_e are the direct and exchange Slater integrals, respectively.

The energy levels were calculated using an atomic-structure program furnished to us by Cowan.[9] The average energies of the various configurations and the spin-orbit and electrostatic parameters were computed from center-of-gravity HFR wave functions.

III. RESULTS AND DISCUSSION

An energy-level diagram showing the relative positions of the configurations $2p^53snl$ ($n = 3,4$; $l = 0,1,2$) in Al^{2+} relative to the ionization threshold is shown in Fig. 1. With the exception of $2p^53s\,3p$, the total separation of levels within a configuration is approximately equal to a typical experimental energy spread of 1 to 2 eV. Although cross sections to individual LS terms within a configuration were calculated, we report here only total cross sections determined by summing over the contributions from each term; the eigenvectors are not pure in LS coupling, and the additional effort involved in an intermediate coupling calculation was not warranted in light of the small energy spread within configurations.

The results of our calculations of the center-of-gravity energies and ionization cross sections at threshold for Mg^+, Al^{2+}, and Si^{3+} are shown in Table I. For comparison, we have also listed the corresponding values in Fe^{15+} as calculated by J. B. Mann.[10] In all cases, the ionization cross sections at threshold were calculated by extrapolating

the collision strengths, calculated at energies above threshold back to threshold.

Our results indicate that the largest contribution to autoionization for Mg^+, Al^{2+}, and Si^{3+} should arise from the $2p \rightarrow 3p$ excitation; however, the relative importance of this transition decreases with ionization stage, and Mann's results indicate that with Fe^{15+} the $2p \rightarrow 3p$ transition contributes only half as much as the dipole allowed $2p \rightarrow 3d$ excita-
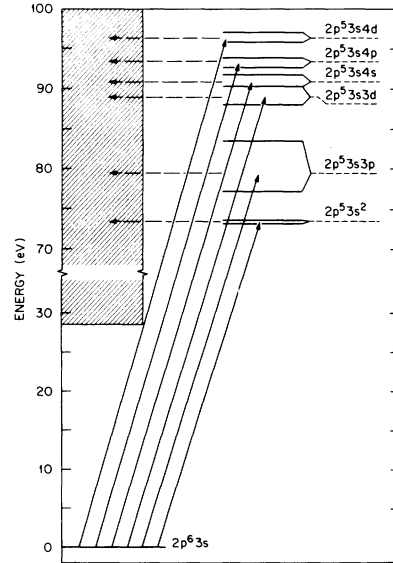
FIG. 1. Energy-level diagram showing the $2p^53snl$ configurations of Al^{2+} with respect to the ionization threshold.

TABLE I. Excitation cross sections at threshold.

Transition	Mg$^+$ ΔE(eV)	Mg$^+$ $\sigma(10^{-18}$ cm^2)	Al^{2+} ΔE(eV)	Al^{2+} $\sigma(10^{-18}$ cm^2)	Si^{3+} ΔE(eV)	Si^{3+} $\sigma(10^{-18}$ cm^2)	Fe^{15+} [a] ΔE(eV)	Fe^{15+} [a] $\sigma(10^{-18}$ cm^2)
$2p \rightarrow 3s$	50.0	0.87	73.2	0.46	100.3	0.25	712.7	0.004
$2p \rightarrow 3p$	54.2	6.02	79.3	4.18	108.2	2.94	752.5	0.126
$2p \rightarrow 3d$	60.4	1.31	88.9	2.00	121.1	2.10	802.7	0.232
$2p \rightarrow 4s$	60.3	0.26	90.8	0.15	126.5	0.09		
$2p \rightarrow 4p$	61.9	1.08	93.2	0.82	129.8	0.57	972.1	0.023
$2p \rightarrow 4d$	63.7	0.61	96.2	0.86	134.0	0.82	989.6	0.052

[a]Determined from J. B. Mann's distorted-wave exchange calculations of collision strengths as reported in Ref. 10. Our values for the $2p \rightarrow 3p$ and $2p \rightarrow 3d$ transitions in Fe^{15+} are in good agreement with the values reported here.

tion. This is consistent with Moore's and Nussbaumer's calculation for Mg$^+$, and the difference between their result for $2p \rightarrow 3p$ of 4.4×10^{-18} cm^2 and our value of 6.0×10^{-18} cm^2 is due primarily to our inclusion of exchange in the cross section, rather than the distortion in our continuum wave functions: If we include only the direct terms in calculating this cross section, we obtain a value of 3.9×10^{-18} cm^2. The reason for this can be seen from Eqs. (8), (9), and (10). Exchange provides the only contribution to transitions to $L_f = 1$ terms since the 3-j symbol

$$\begin{bmatrix} 1 & L_f & 1 \\ 0 & 0 & 0 \end{bmatrix}$$

vanishes for $L_f = 1$ and the values of R_d^2 are small so that exchange provides the major contribution to transitions to $L_f = 2$ terms. Thus, exchange increases the total cross section.[11] It is also worth noting that $\approx 90\%$ of this cross section in Mg$^+$, Al^{2+}, and Si^{3+} is due to three direct monopole terms for $l_i = 0, 1, 2$ and one exchange monopole term for $l_i = 1$.

Comparisons between our calculations and the experimental results of Crandall et al.[5] for Mg$^+$, Al^{2+}, and Si^{3+} are shown in Figs. 2, 3, and 4. In order to provide a reliable estimate of the indirect process we must calculate the direct process as accurately as possible. This we did by taking Younger's fit to his distorted-wave calculations for the Na isoelectronic sequence[12] and scaling it to the experimental values before the onset of autoionization. The resulting direct cross sections are shown by the dashed curves. The solid curves are the sums of our values of σ_{excit} and the cross sections for the direct process.

It is immediately obvious that the distorted-wave

calculations overestimate the total contribution of excitation autoionization in all three elements by about a factor of 2. By comparing experiment with theory in Al^{2+} where the indirect process shows a number of resolved resonant structures and the experimental results are more accurate than in Si^{3+}, one sees that the largest discrepancy appears to be in our calculation of the contribution of the $2p \rightarrow 3p$ transition. The data points within the energy range from 77.1 to 83.5 eV, where the energy levels of $2p^5 3s\,3p$ occur, indicate that the contribution from this transition is less than 0.7×10^{-18} cm^2 rather than our calculated value of 4.2×10^{-18} cm^2.

One possible explanation of this apparent
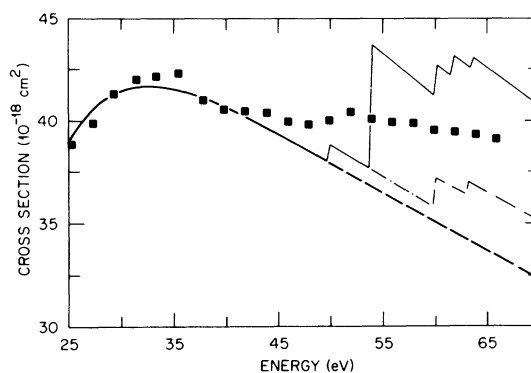
FIG. 2. Ionization cross section of Mg$^+$: blacked square—experimental results (Ref. 5); dashed curve—Younger ionization equation scaled to the data before the onset of the indirect processes (required scale factor of 0.78); solid curve-direct ionization curve + distorted-wave excitation cross sections for $2p^6 3s \rightarrow 2p^5 3snl$ ($n = 3, 4$; $l = 0, 1, 2$); dot-dashed curve—direct-ionization curve + distorted-wave excitation cross sections excluding $2p \rightarrow np$ excitations.
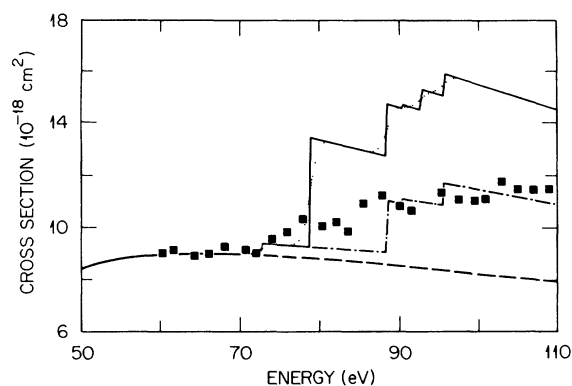
FIG. 3. Ionization cross section for Al^{2+}: blacked square—experimental results; dashed curve—Younger ionization equation normalized to experimental data before the onset of the indirect process (required scale factor of 0.65); solid curve—direct-ionization curve + distorted-wave excitations cross sections for $2p^63s \rightarrow 2p^53snl$ ($n = 3,4$; $l = 0,1,2$); dotted curve—solid curve convoluted with 2-eV FWHM Gaussian to simulate experimental energy spread; dot-dashed curve—direct-ionization curve + distorted-wave excitation cross sections excluding $2p \rightarrow np$ excitations.

discrepancy is nonunit branching ratios for autoionization from levels of $2p^53s\,3p$. Our calculations indicate that, unlike the other configurations considered here, some of the levels of $2p^53s\,3p$ (and
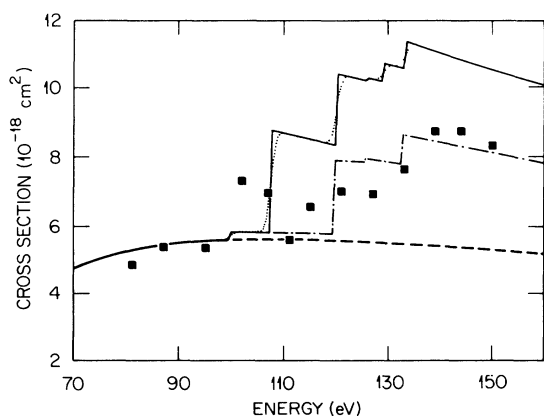
FIG. 4. Ionization cross section for Si^{3+}: blacked square—experimental results; dashed curve—Younger ionization equation (in this case, the equation fit the data before the onset of the indirect process, and no scaling was required); solid curve—direct-ionization curve + distorted-wave excitations cross sections for $2p^63s \rightarrow 2p^53snl$ ($n = 3,4$; $l = 0,1,2$); dotted curve—solid curve convoluted with 2-eV FWHM Gaussian to simulate experimental energy spread; dot-dashed curve—direct-ionization curve + distorted-wave excitation cross sections excluding $2p \rightarrow np$ excitations.

to a lesser extent $2p^53s\,4p$) have branching ratios appreciably less than 1. This is due primarily to selection rules for autoionization from various LS terms which are of higher purity in $2p^53s\,3p$ than in the other configurations. For example, if the $2p^53s(^{1,3}P)3p\ ^2P$ terms are pure, they cannot autoionize to the continuum states $2p^6kl$ and still conserve parity. However, these terms can radiate to levels of the bound-state configuration $2p^63p$. Furthermore, if the quartet terms are pure, they can neither autoionize to the doublet states in the continuum nor radiate to the doublet states of $2p^63p$. However, the ^2S terms, which have the largest excitation cross sections, also have high autoionization rates to the continuum, and nearly unit branching ratios. Thus, the effect of non-unit branching ratios is relatively small. We have estimated that if the ^2P and ^4L_f terms were pure, this could reduce the contribution of the $2p^53s\,3p$ configuration by as much as 30%. With the amount of mixing predicted by our calculation, this reduction would be more like 15%.

We have also considered the effects of configuration interaction on the $2p^53s\,3p$ configuration; however, such effects were found to be small in all three elements, and a single-configuration calculation appears to provide a good approximation. Assuming that interference between the direct and indirect processes is small, we are thus led to the conclusion that both the Coulomb-Born and the distorted-wave approximations substantially overestimate the size of the $2p \rightarrow 3p$ (and apparently also the $2p \rightarrow 4p$) excitation cross sections which, from our earlier discussion, implies that both approximations yield monopole terms that are simply too large.

Also shown in Figs. 2, 3, and 4 are curves for the total cross sections which exclude the excitation-autoionization contributions from $2p^53s\,3p$ and $2p^53s\,4p$. In the case of Al^{2+}, the agreement between this curve and the experimental results is much better, at least with regard to the magnitude of the overall contribution of the indirect process. However, there are also some pronounced discrepancies beyond the rather small but measurable contribution from the $2p^53s\,3p$ configuration. The three data points between 84 and 88 eV indicate a contribution of $\simeq 1.5$ to 2.0×10^{-18} cm^2 which begins about 4 eV before the onset of the $2p \rightarrow 3d$ excitation. There are two possible explanations for this. The $2p^53p^2$ configuration is centered at 87.5 eV and has levels with energies as low as 85.3 eV. A number of levels from this con-

figuration mix rather strongly with levels from $2p^5 3s\, 3d$, and such interactions could account for at least some of this apparent resonance. A second possibility is the process of double Auger ionization introduced recently by LaGattuta and Hahn[13] in Fe^{15+}. In this process, the initial ion (Z,N) in the ground state captures an incoming electron with the simultaneous excitation of an inner-shell electron, forming a doubly excited state of $(Z,N+1)$ (e.g., $k_i l_i + 2p^6 3s \rightarrow 2p^5 3s\, 3dnl$). This state may then undergo two sequential Auger emissions forming $(Z,N-1)$ in its ground state. LaGattuta and Hahn's calculations indicate that this process adds a substantial resonance contribution below the $2p \rightarrow 3d$ transition in Fe^{15+} and, therefore, this same process may account for this apparent resonance below the $2p \rightarrow 3d$ excitation in Al^{2+}. Double Auger ionization might also account for the data points between 75 to 78 eV before the onset of the $2p \rightarrow 3p$ transition.

The experimental results for Si^{3+} are not sufficiently precise to make any detailed comparisons. However, it should be noted that the apparent total contribution of excitation autoionization above 140 eV agrees well with the theoretical curve, excluding the $2p \rightarrow np$ excitations. The data for Mg^+ show a departure from the direct-ionization curve well before the calculated energy of the $2p^5 3s^2$ configuration, and no abrupt increases can be seen in the energy range where the various resonances are expected to occur. The lack of any well-defined resonant structures is difficult to understand in terms of our calculations. However, the calculated positions of the autoionizing configurations are closer together than in the cases of Al^{2+} or Si^{3+} and the energy spread within each configuration is about the same. The latter combined with the experimental energy spread (expected to be only 0.5 eV in Mg^+), as well as the possibility of double Auger resonances between each of the autoionizing configurations, may leave the total pattern unresolved. In addition, interference between the direct and indirect ionization processes may have some effect. However, none of these effects appear to be large enough to account for the gradual departure between the data and the calculation of the direct process which appears to begin between 42 and 45 eV, rather than near the position of the $2p^5 3s^2$ configuration at 50 eV. If we assume that the slope in the direct ionization cross section between 40 and 65 eV is accurately predicted by the equation from Younger, we have no explanation for this discrepancy. Finally it should be noted

that, in contrast to the cases of Al^{2+} and Si^{3+}, the experimental Mg^+ data lie nearly midway between the two theoretical curves, rather than close to the theoretical curve which excludes the $2p \rightarrow np$ transitions. This may imply that the $2p \rightarrow np$ excitation-autoionization effects are relatively larger in Mg^+, as is predicted by the distorted-wave calculations.

IV. CONCLUSIONS

Our results indicate that the contribution of excitation autoionization to the ionization cross sections of ions in the Na isoelectronic sequence are overestimated when one adds a distorted-wave excitation cross section to the direct-ionization cross section. The primary discrepancy seems to arise from the $2p \rightarrow 3p$ (and to a lesser extent the $2p \rightarrow 4p$) transition. This is especially apparent in the case of Al^{2+}. However, as we move along the isoelectronic sequence toward Fe^{15+} this discrepancy will most likely decrease since the relative contributions of the $2p \rightarrow np$ excitations are predicted to decrease.

In seeking an explanation for the disagreement between theory and experiment we may consider two possibilities: (1) A deficiency in our independent processes model for the total ionization cross section, as reflected in Eq. (1); (2) assuming the general validity of Eq. (1), a deficiency in our distorted-wave model for the excitation of the monopole-dominated $2p \rightarrow np$ transitions.

To a limited degree the first possibility has been investigated by recent studies of the quantum-mechanical interference between the direct and excitation-autoionization processes. Both close-coupling[14] and perturbation[15] theories have been used to include interactions between inner-shell autoionization states and the ejected electron continuum. For Li-like C^{3+}, N^{4+}, O^{5+}, and Zn-like Ga^+ the inclusion of interference has been found to have a quite small effect on the total-ionization cross section. Although a more general ionization theory would also include incident electron capture to doubly excited autoionization states[13] as well as post-collision interactions,[16] we feel that Eq. (1) is generally valid for electron-impact ionization of the atomic ions considered in this paper.

Further theoretical and experimental research is needed in order to pass judgement on the second possibility. We suggest that experimental measurements should be made on monopole-dominated

$2p \rightarrow np$ transitions in which the upper state is truly bound. This would simplify the application of either distorted-wave or close-coupling theory to the problem. It is perhaps worth noting that the outstanding discrepancy between theory and experiment in the field of inelastic scattering of electrons by simple ions concerns the He^+ $(1s \rightarrow 2s)$ cross section,[17] another monopole-dominated transition.

ACKNOWLEDGMENTS

*On sabbatical leave from Rollins College, Winter Park, Florida.

[1]O. Bely, J. Phys. B 1, 23 (1968).

[2]D. L. Moores and H. Nussbaumer, J. Phys. B 3, 161 (1970).

[3]S. O. Martin, B. Peart, and K. T. Dolder, J. Phys. B 1, 537 (1968).

[4]R. D. Cowan and J. B. Mann, Astrophys. J. 232, 940 (1979).

[5]D. H. Crandall, R. A. Phaneuf, R. A. Falk, and G. H. Dunn, Phys. Rev. A 25, 143 (1982), (paper I).

[6]R. D. Cowan, Phys. Rev. 163, 54 (1967).

[7]R. D. Cowan and D. C. Griffin, J. Opt. Soc. Am. 66, 1010 (1976).

[8]M. E. Riley and D. G. Truhlar, J. Chem. Phys. 63, 2182 (1975).

[9]The atomic-structure program is described in R. D. Cowan, The Theory of Atomic Structure and Spectra (University of California Press, Berkeley, 1981).

[10]A. L. Merts, J. B. Mann, W. D. Robb, and N. H. Magee, Jr., Los Alamos Scientific Laboratory Report No. LA-8267, 1980 (unpublished).

[11]The contribution of exchange may be reduced in some cases by including the term in the reactance matrix which results from the lack of orthogonality between the bound state spin orbitals of the active electrons and the continuum wave functions with equal angular momentum. We have calculated this for the $2p \rightarrow 3p$ excitation in Mg^+, Al^{2+}, and Si^{3+} and have found that it reduces the total cross sections by either 3% or 10% depending on whether we use the post or prior forms, respectively. In making this calculation, we have used the form of this term employed by Mann and given in R. E. H. Clark, N. H. Magee, Jr., J. B. Mann, and A. L. Merts (unpublished).

[12]S. M. Younger, Phys. Rev. A 24, 1272 (1981).

[13]K. J. LaGattuta and Y. Hahn (private communication).

[14]H. Jakubowicz, Ph.D. thesis, University of London, 1980 (unpublished).

[15]M. S. Pindzola, D. C. Griffin, and C. Bottcher, Phys. Rev. A 25, 211 (1982).

[16]H. G. M. Heidman and W. Van de Water, Comments At. Mol. Phys. 10, 87 (1981).

[17]For a recent review see S. A. Wakid and J. Callaway, J. Phys. B 13, L605 (1980).